IJCRT.ORG ISSN : 2320-2882

INTERNATIONAL JOURNAL OF CREATIVE RESEARCH THOUGHTS (IJCRT)

An International Open Access, Peer-reviewed, Refereed Journal

Synthesis and Characterization of Zeolite-Y encapsulated [Tyr-M(II)-His] ternary complexes

Janapati Srinu[1], Dr. M. Radhika[*1],

[1]Department of Chemistry, Nizam College, Osmania University, Hyderabad, 500001, India.

Abstract: Nanocavity Zeolite Y Encapsulated M(II) (M= Co, Ni, Cu & Zn) ternary complexes of L-Tyrosine and L-Histidine in situ in Na-Y Zeolites were synthesized using the ion exchange and flexible ligand methods. Initially, the metal ions were introduced into the zeolite framework through ion exchange with Na^+ ions, followed by diffusion of the amino acid ligands tyrosine and histidine into the super cages of the zeolite, where coordination with the metal centers occurred to form encapsulated ternary complexes by the reaction of ion exchanged process and flexible ligand method. The geometry and binding modes were explained by using various characterization techniques such as TGA, XRD, ESR, SEM, EDX, UV and IR spectroscopy.

Key words: Zeolite-Y, L-Tyrosine, L-Histidine, Flexible ligand synthesis, Encapsulation

1. Introduction

The zeolites have a crystalline structure made up of connected tetrahedra and they have open voids that look like channels and cages. Water molecules and various cations that can be exchanged commonly fill them. This definition has undergone significant modifications over time [1], resulting in the following observations: (a) the tetrahedral (T) position in the framework may be occupied by cations other than Si and Al, such as Be, P, Zn, or others; (b) even anhydrous and/or non-exchanging minerals can be classified as zeolites; and (c) a continuous tetrahedral framework allows for certain interruptions. Considering all of this, zeolites are well-known for their well-organized matrices, which have nanopores and nanochannels that can hold different things. Zeolites can lose water and then take it back in without breaking or changing the size of the structure [2-4]. The three-dimensional catenation of several basic tetrahedral units makes up the crystalline structure. Each unit has an oxygen atom, while the center has an aluminium or silicon atom. Through the amine and carboxylate moieties, the amino acids create stable five-membered chelates with different metal ions (N, O-chelation). Several amino acids have an additional metal binding site in the side chain and thus form metal complexes with a variety of structures. Important metal binding sites in proteins include the thiol group of cysteine (Cys), the imidazole ring of histidine (His), the phenol ring of tyrosine (Tyr) [19].

The amino acid derivative has been used as a catalyst for the hydrolysis of esters because it can form complexes with transition metals. After complexation, the metal complexes made from amino acids prevent the growth of bacterial and fungal strains and form stable complexes with transition metals [20]. Additionally, the preparation of functional metal nanoparticles that were used in various scientific applications was revealed by some of the studies. Tin homometallic complexes were synthesized, and their antimicrobial properties were examined and documented, yielding better results for metal complexes with ligands [21]. Additionally, the synthesis of metal complexes containing Co, Ni, Cu and Zn was suggested, along with their structural clarification and anticorrosion application. In continuation of zeolite encapsulated [Tyr-M(II)-His] ternary complexes. Later on, to study the catalysis of these encapsulated

complexes in various reactions like decomposition of H_2O_2, oxidation of phenol etc. Further, the properties of the prepared metal complexes of amino acids with zeolite Y nano materials were investigated using various kinds of analytical technique such as UV, IR, XRD, ESR, SEM, EDX and TGA.

2. Experimental

2.1 Materials

M(II) nitrates (M=Co, Ni, Cu & Zn), tetrahydrofuran and DMF are obtained from Merck (GR grade). Na-Y Zeolite with Si:Al ratio of 5:1 are purchased from Aldrich, while ethanol, methanol, N, N-Dimethyl formamide, Tyrosine and Histidine are purchased from Sigma-Aldrich. All these commercially available reagents obtained were used without any further purification.

2.2 Synthetic methods:

2.2.1 Synthesis of the encapsulated complex was carried out by employing two steps

Step 1: Preparation of metal exchanged Na-Y Zeolite: M(II)-Y

The ion exchange process was utilised to swap metal ions with Na ions in zeolite Y. In 100 cm^3 of deionised water, 2 g of Na-Y zeolite is added. Then, MNO_3 (0.025M) (M=Co, Ni, Cu & Zn) was added to this and the mixture is gently stirred at 90 °C for 24 hours. The precipitate is filtered and washed with sufficiently hot deionised water until the filtrate is free from Na ions. Then, the precipitate is dried in a hot-air oven at 100 ^oC for 10 hours.

Step 2: Synthesis of [Tyr-M(II)-His]-Y Encapsulated Ternary Complexes

For the production of Zeolite Y encapsulated ternary complexes utilised flexible ligand synthesis. Add 0.775 g of L-Histidine (dissolved in 100cm^3 of methanol) to a stirred solution of methanol and M(II) Zeolite Y. After 8 hours of refluxing, the solid complex was filtered, washed with ethanol and dried in a hot air oven at 80 ^oC for 14 hours. Then add 2g of this binary complex in 100 cm^3 of methanol with 0.905 g of L-Tyrosine and refluxed for 24 hours. The precipitate is filtered and then extracted with DMF and ethanol in a soxhlet for around 3 to 4 hours to remove the additional compounds that are adsorbed on the zeolite. After soxhlet extraction, the final product is dried in a hot air oven at 90 °C for 12 hours [16].

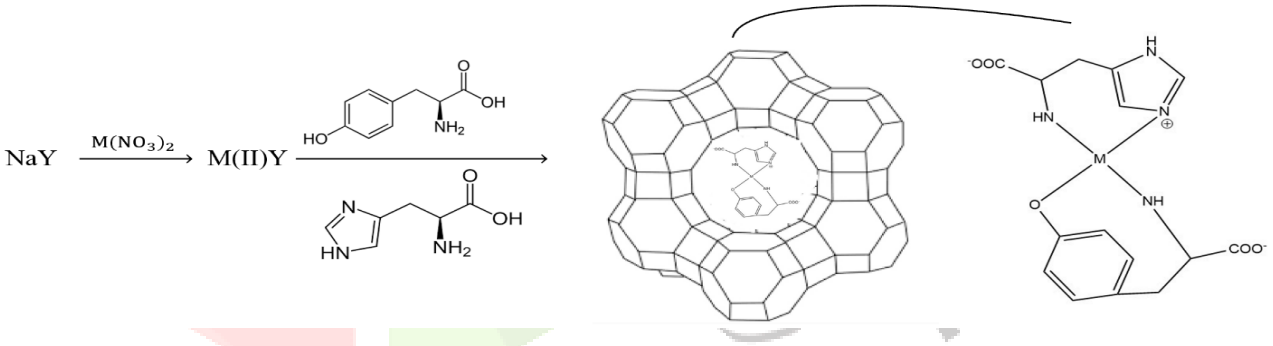

Scheme 1. Synthesis of encapsulated ternary metal complexes [Tyr-M(II)-His]-Y [M(II) = Co, Ni, Cu & Zn]

2.2.3. Characterization

The Zeolite encapsulated [Tyr-M(II)-His] ternary complexes are characterized using UV-Vis spectrophotometer Shimadzu UV-1900i/1280 to study the concentration and assess purity of synthesized ternary metal complexes. The FT-IR spectra of the complexes was done using the KBr disc method on an FT-IR DIGILAB Biorad spectrometer. The powder X-ray diffraction (XRD) of the complexes was recorded using Ni filtered CuKα radiation (λ=1.5406 A^o) in the scan range of 10-80^o on a Rigiku Miniflex (Rigaku Corporation, Japan) X-ray diffractometer. The FE-SEM images and EDX analysis of zeolite encapsulated [Tyr-M(II)-His] ternary complexes were captured using a JEOL FE-SEM-7610F microscope. In addition, the TGA analysis was carried out by using NETZSCH TG 309 Libra. The ESR analyzer Ali Fax Roller 20 LC was used to find the co-ordination geometry of [Tyr-M(II)-His] ternary complexes.

3 Results and discussion

3.1 Characterization techniques

The optical properties of the synthesized Zeolite encapsulated [Tyr-M(II)-His] ternary complexes were studied by UV–Vis DRS absorption. An absorption peak could be found at 200 – 400 nm in the UV-Vis Diffuse reflectance Spectroscopy (UV-Vis DRS) for all [Tyr-M(II)-His]-Y (Tyrosine-Metal (II)-Histidine-Y) complexes., which primarily indicates the presence of transitions in the aromatic side chains of amino acids and typically indicate the presence of aromatic amino acid residues of Histidine and tyrosine and their

interaction with the metal ion. Ligand-induced transitions were predominantly observed in the ultraviolet (UV) region, while d−d transitions were noted in the visible region. In the case of [Tyr-M(II)-His]-Y (M=Co, Ni, Cu and Zn) metal complexes clear absorption bands showed at 214 and 271 nm, these corresponding to $\pi - \pi^*$ transition. The UV-vis spectrum also showed another low-intensity peak between 347 and 442 nm. This peak could be linked to the $n \rightarrow \pi^*$ ($^4A_2F \rightarrow {}^4T_1F$) and $n \rightarrow \pi^*$ ($^4A_2F \rightarrow {}^4T_1P$). The bands 500-600 nm region indicates the d-d transition states, which suggests that the cobalt (II) ion has a square planar geometry structure. The magnetic moment of the Co (II) complex was computed to be 4.48 μB, which corresponds to the anticipated square planar geometry [19]. The d−d transition does not occur in the Zn [Tyr-Zn (II)-His-Y] complex, due to the absence of unpaired electrons (d^{10} configuration)

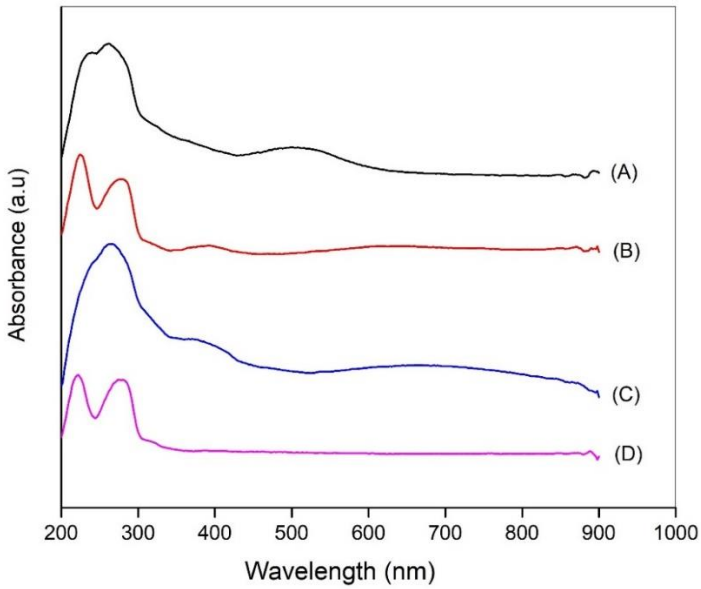

Figure 1: UV-Vis spectra of (A) [Tyr-Co (II)-His]-Y, (B) [Tyr-Ni (II)-His]-Y, (C) [Tyr-Cu (II)-His]-Y, (D) [Tyr-Zn (II)-His]-Y

FT-IR was utilized to find the functional groups in the synthesised zeolite encapsulated [Tyr-M(II)-His] ternary complexes. The results are shown in Figure.2. The less strong IR peaks show that the complexes are trapped in the zeolite matrix. The FTIR spectra of both parent zeolite and metal-exchanged zeolite exhibit pronounced bands within the range of 450-1200 cm^{-1}. There is a strong and wide band around 1020 cm^{-1} that shows asymmetric stretching vibrations of $(Si/Al)O_4$ units of zeolite. There are some wide bands close to 3420 cm^{-1} that are likely caused by lattice water molecules [18].

The IR spectra of encapsulated complexes (Table 1) indicate no shift in the zeolite lattice bands (1020 cm^{-1}). This means that the zeolite framework has not changed after it was encapsulated. The bands between 1200 and 1600 cm^{-1} show that there is coordination in the pores, where zeolite does not have any bands. But these bands aren't as strong because the encapsulated complexes aren't as concentrated in the lattice. The shift in the distinctive bands of carboxylic acids after coordination is also looked at. Amino acids in their free state exist as zwitterions, having two vibrations, one for $vsCOO^-$ and one for $vasCOO^-$, that are about 1412 and 1606 cm^{-1} and NH_3^+ shows vibrations at 3094 cm^{-1}.

The Vs and Vas of COO^- (Fig 2) in the encapsulated complexes do not show any shifts in the stretching frequency confirming that $-COO^-$ is not involved in metal coordination (M=Co, Ni, Cu and Zn). The Phenolic -OH peak present in the free tyrosine does not appear in the metal complexes indicating that metal ion is binds to the phenolic -OH group of tyrosine.

The νNH_3^+ in an amino acid usually shows up between 3094 and 3078 cm^{-1} for tyrosine and histidine respectively. The bands of νNH_2 at 3128, 3147, 3128, and 3126 cm^{-1} confirmed the bonding with Co, Ni, Cu and Zn (II) metal ions, respectively. The free histidine contains imidazole peak at 1579 cm-1, which is shifted to higher frequency (1589-1591 cm-1) indicating that imidazole nitrogen binds to the metal ion. The IR data clearly indicates that the coordination number is four around the metal ion in the synthesized ternary complexes. Which indicating that the synthesized amino acid metal complexes exhibited square planer complexes.

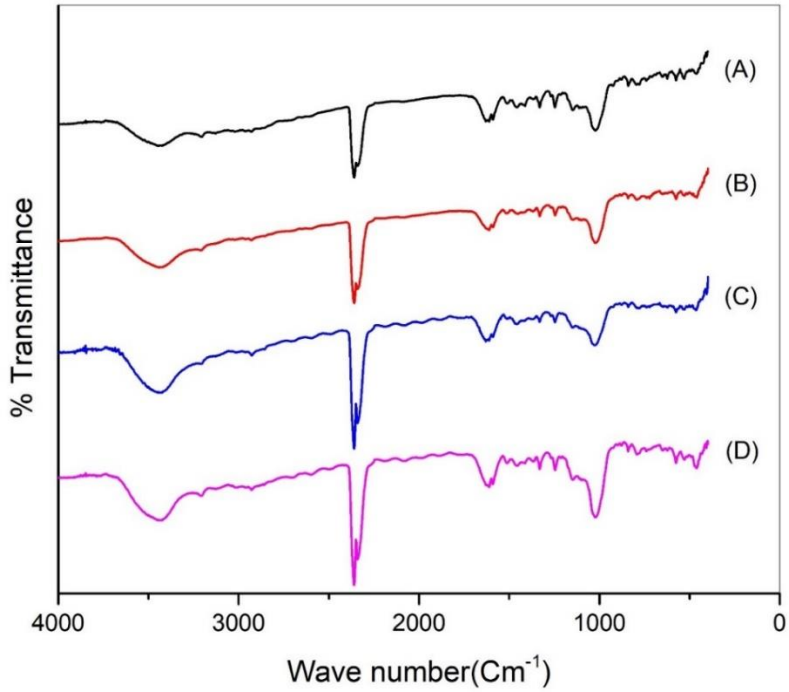

Figure 2: FTIR spectra of (A) [Tyr-Co (II)-His]-Y, (B) [Tyr-Ni (II)-His]-Y, (C) [Tyr-Cu (II)-His]-Y, (D) [Tyr-Zn (II)-His]-Y

Table 1. FT-IR Vibrational spectra of L-tyrosine (Tyr), L-Histidine and of the [Tyr-M-His]-Y (M=Co, Ni, Cu and Zn) complexes

Assignment	Free L-Tyrosine	Free Histidine	Tyr-M-His-Y (M=Co, Ni, Cu, Zn)			
	IR	IR	Co	Ni	Cu	Zn
$\nu_{as}(NH_2)$			3205	3207	3205	3205
$\nu_s(NH_2)$			3128	3147	3128	3126
$\nu_{as}(NH_3^+)$	3094 vs	3078	-	-	-	-
$\nu_{as}(COO^-)$	1589 vs	1606	1610	1610	1610	1610
$\delta(NH_2)$			1625	1621	1631	1627
ν(C=O)			1591	1585	1564	1545
$\delta(NH_3^+)$	1668 w					
$\delta(CH_2)$	1459 s	1450	1447	1451	1449	1484
$\nu(COO^-)$	1412 vs	1412	1411	1425	1411	1411
ν(OH)Tyrosine	3657	-	-	-	-	-
δ(CH)	1317 m		1324	1327	1322	1314
ν(C–N) aliphatic	1097 s	1062	1085	1078	1087	1087
$\delta(COO^-)$	743 vs		729	720	728	725
ν(C=N) (Imadazole)		1579	1591	1589	1589	1591
ν(M–N)			454	452	4554	462
Zeolite (Si-O-Al			1022	1020	1026	1022

The X-ray diffraction technique was employed to learn about the structure of the synthesized encapsulated ternary complexes. The results are shown in Figure 3. At 2θ = 10.3°, 15.9°, 18.6°, 23.9°, 27.4°, and 31.6°, all of the materials exhibited distinct peaks in their XRD patterns. The (2 2 0), (3 3 1), (4 4 0), (5 5 3), (6 4 2), and (7 5 1) planes were found to reflect Na-Y zeolite [20]. There were no other peaks in the XRD patterns that were associated to metal ions. This means that the [Tyr-M(II)-His]-Y ternary complexes that are inside the zeolite are well spread out in the zeolite cavities. So, the conditions around the zeolite host do not affect its crystallinity.

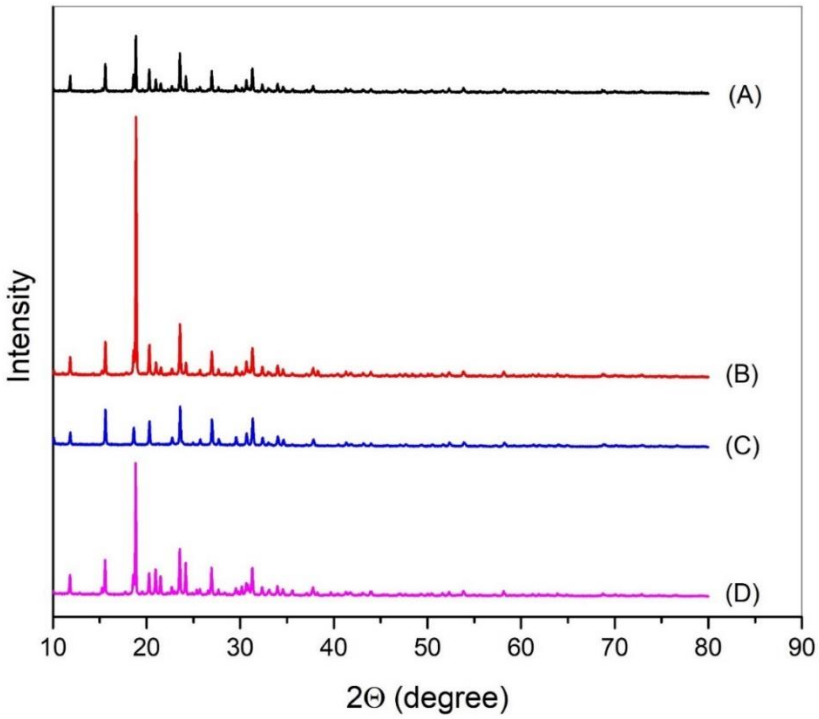

Figure 3: XRD Pattern of (A) [Tyr-Co (II)-His]-Y, (B) [Tyr-Ni (II)-His]-Y, (C) [Tyr-Cu (II)-His]-Y, (D) [Tyr-Zn (II)-His]-Y

The X band ESR spectra of encapsulated Co (II) and Cu (II) Complexes were documented at ambient temperature and is displayed in Fig.4. The ESR spectrum shows that copper and cobalt complexes are encapsulated. The spectra showed clear hyperfine structure of the zeolite-encapsulated species, which is typical of isolated monomeric Cu (II) and Co (II) complexes. The encapsulated metal complex is isolated in the diamagnetic zeolite matrix, where intermolecular interactions are avoided, allowing for the observation of resolved hyperfine structures. "The ESR spectrum pattern of the solid copper (II) complex exhibits an axial type symmetry (Table 2), where g// > g⊥>2.0023, indicates that the structure of the complex is square planar and the unpaired electron is in d(x^2-y^2) orbital. In square planar complexes with an electron in d(x^2-y^2) orbital gives $2B_{1g}$ as the ground state [21]. The high covalence property of the complex with distorted symmetry is suggested by the calculated = (g// + 2g⊥)/3 = 2.17 value [22]. The g-values are related by G= (g//−2.003)/(g⊥−2.003) = 4.0 in an axial symmetry and if G>4 there is a negligible exchange interaction between Cu (II) centres in the solid state and vice-versa. The G value of the copper complex is found to be 11.54, ruling out the exchange interactions [19], supporting the encapsulation and presence of isolated monomeric Cu (II) and Co (II) complexes in zeolite cavities. The stereochemistry of Cu (II) complexes can be evidenced from the (g///A//) values. The range 105 -135 cm^{-1} and >135-250 cm^{-1} are reported for square planar and tetragonal distorted complexes respectively. The copper complex has (g///A// = 108 cm^{-1}), which lies in the range reported for square planar Cu (II) complexes [23]. The cobalt complex has an isotropic g = 4.20, which suggests the distorted octahedral structure. These results agree with magnetic moment values, Cu complex with 1.75 BM (S=1/2) and Co complex with 3.80 BM (S=3/2).

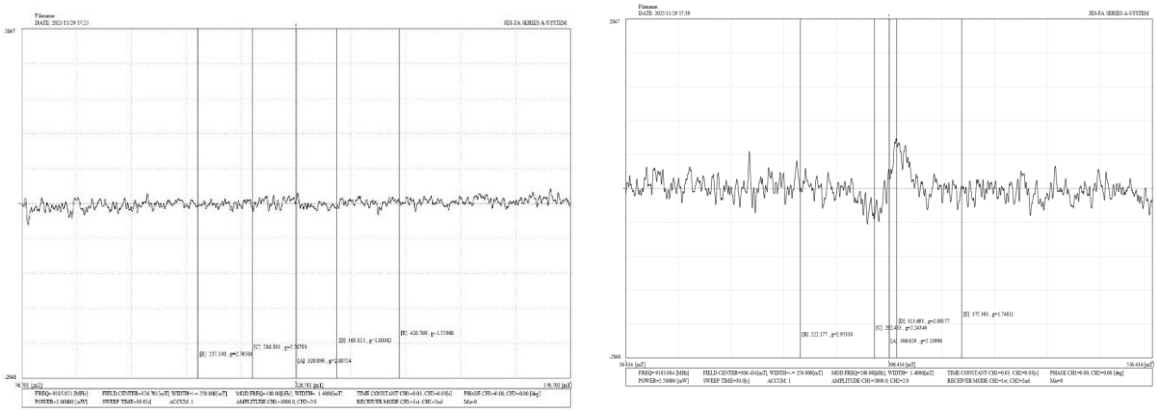

(A) (B)

Figure 4: ESR spectra of **(A)** [Tyr-Co (II)-His]-Y, **(B) [**Tyr-Cu (II)-His]-Y

Table 2: ESR data of zeolite-Y encapsulated Cu (II) and Co (II) ternary complexes

Complex	g//	g⊥	g_{av}	A_l (x10 cm)	$A_\perp$ (x10 cm)	$g_{l/At(cm^{-1})}$
Tyr-Cu-His-Y	2.39	2.05	2.27	227	27	110
Tyr-Co-His-Y	4.19	2.04	2.74	212	23	203

The ternary complexes, all of which were encased in Zeolite and examined using FE-SEM micrographs and EDX analyses, exhibited a faujasite (FAU) framework structure characterised by a cubic crystal system and it can be found in Figures 5 and 6. According to the EDX tests, sodium ions are the main components of the NaY zeolite. They are located in the zeolite framework and on the surface to keep the negative charges from the aluminium stable. Silicon and aluminium, which are also parts, have tetrahedral interactions with oxygen. The formation of [Tyr-M(II)-His]-Y ternary complexes altered the NaY zeolite. When organic molecules bind with different metal complexes, the carbon content of the complexes went from 44.1% to 7.84%. Table 2 shows the EDX elemental composition of ternary metal complexes of [Tyr-M(II)-His]-Y in detail. It includes the Si/Al ratio and the Na (wt %) content. For the most part, the Si/Al ratios of [Tyr-M(II)-His]-Y ternary complexes are similar those of the original NaY zeolite. The results show that the surface deposits have been eliminated, and the scanning electron microscopy images taken after soxhlet extraction show the zeolite surface boundaries clearly. This clearly shows that complexes have been trapped [24].

Table 2. EDX elemental percentages of **[**Tyr-M(II)-His]]-Y ternary metal complexes

Element	**Zeolite**	**[Tyr-Co-His]-Y**	**[Tyr-Ni-His]-Y**	**[Tyr-Cu-His]-Y**	**[Tyr-Zn-His]-Y**
C	44.1	28.26	15.56	7.84	24.40
N	-	30.26	4.20	2.47	7.24
O	37.62	25.91	42.52	48.27	38.55
Na	3.21	1.84	2.89	4.81	2.84
Al	3.33	2.73	7.54	8.68	6.20
Si	9.97	9.41	22.39	24.12	19.12
Si/Al	3.21	3.23	2.79	2.89	3.14
Metal	-	2.17	5.69	3.74	3.81

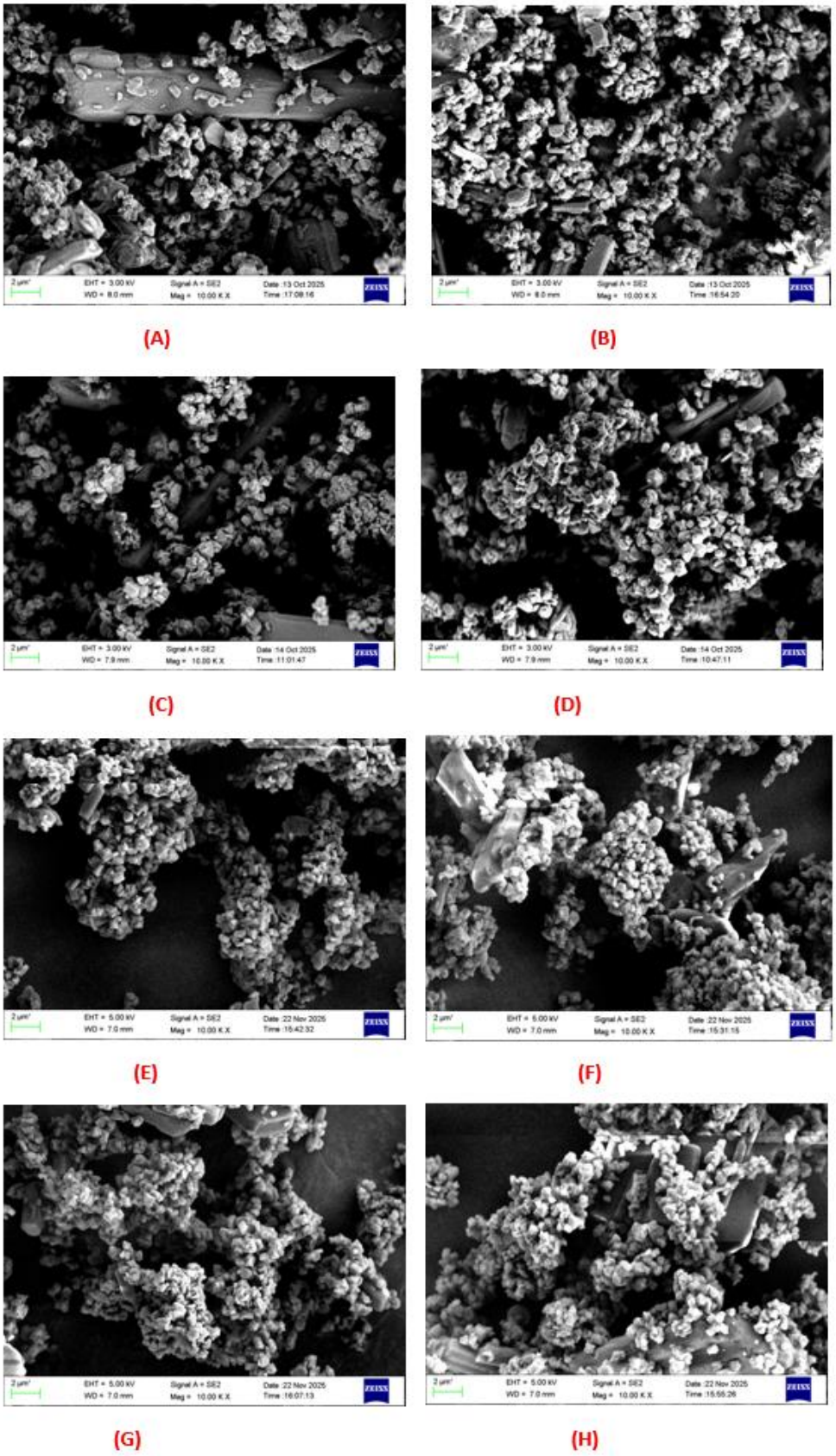

Figure 5: FE-SEM Images of (A)[Tyr-Co (II)-His]-Y BS (B)[Tyr-Co (II)-His]-Y AS (C) [Tyr-Ni (II)-His]-Y BS (D) [Tyr-Ni (II)-His]-Y AS (E) [Tyr-Cu (II)-His]-Y BS (F) [Tyr-Cu (II)-His]-Y AS (G) [Tyr-Zn (II)-His]-Y BS (H) [Tyr-Zn (II)-His]-Y AS

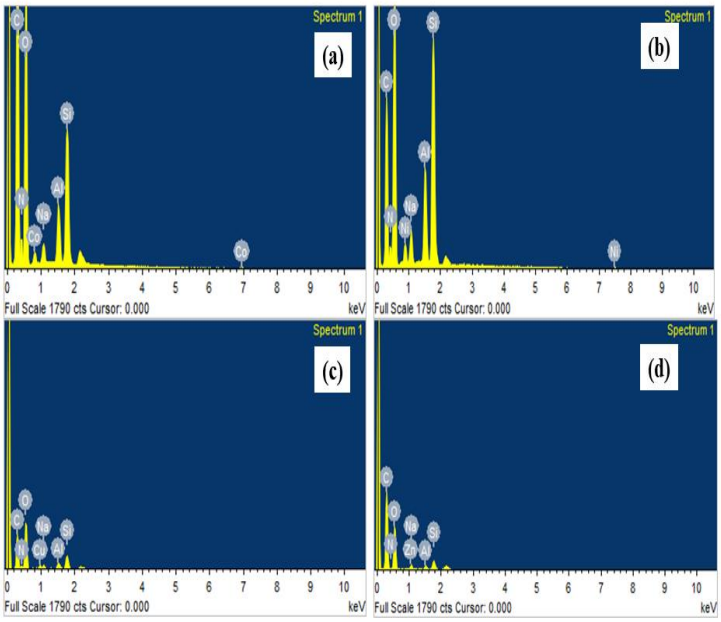

Figure.6. EDX elemental analysis of (A) [Tyr-Co (II)-His]-Y (B) [Tyr-Ni (II) His]-Y (C) [Tyr-Cu (II)-His]-Y (D) [Tyr-Zn (II)-His]-Y

Fig. 7 shows the results of thermogravimetric analysis (TGA) and DTA, which were conducted from room temperature to 1000 °C. [Tyr-M(II)-His]-Y ternary complexes' TGA profile. The first weight loss below 210 °C is mainly caused by the evaporation of moisture and highly volatile compounds. The breakdown of Tyr and His anions and co-intercalated nitrate, as well as the dihydroxylation of the brucite-like layers, cause the second one (250–400 ^{o}C), which involves a progressive loss of weight. The third one, where the combustion of the carbonaceous residue causes a corresponding exothermic reaction and a sharp weight loss in the 400–800 ^{o}C temperature range [25].

Fig. 7 showed the [Tyr-M(II)-His]-Y ternary complexes DTA curves and TGA curves. Four steps make up the thermal breakdown of [Tyr-M(II)-His]-Y: the first occurs between 20 and 150 ^{o}C and is caused by the removal of surface and interlayer water; the second occurs between 150 and 250 ^{o}C and is related to the dihydroxylation of the host layers with a weak endothermic reaction. Tyr and His ions breakdown are responsible for the third weight loss step (260–400 ^{o}C), while the carbonaceous residue burning is responsible for the final one (400–800 ^{o}C) [26].

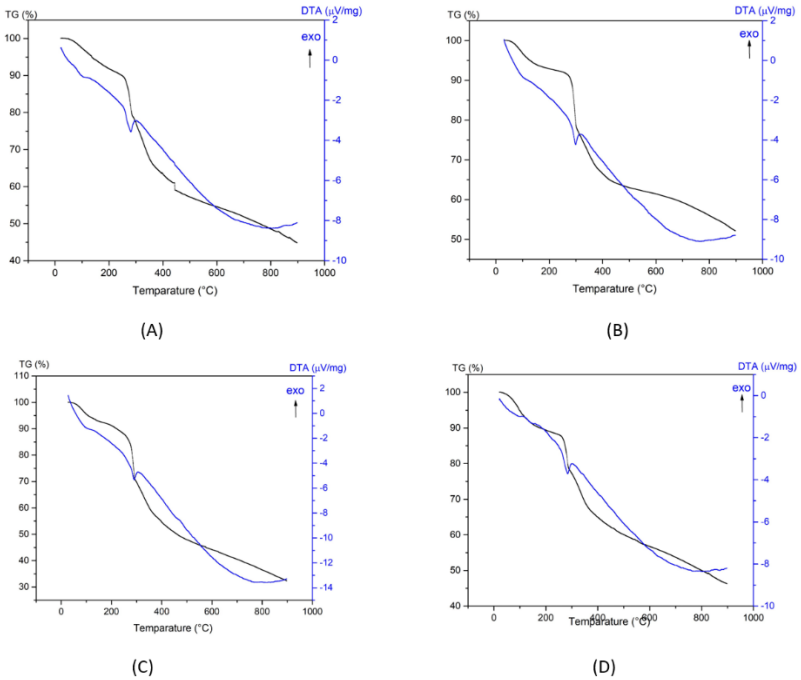

Figure 5: TG-DTA of **(A)** [Tyr-Co (II)-His]-Y, **(B)** [Tyr-Ni (II)-His]-Y, **(C)** [Tyr-Cu (II)-His]-Y, **(D)** [Tyr-Zn (II)-His]-Y

4 Conclusion

The Nanocavity Zeolite Y Encapsulated M(II) (M= Co, Ni, Cu, Zn) ternary complexes of Tyrosine and Histidine in situ in Na-Y-Zeolites were successfully synthesized using the ion exchange and flexible ligand method. Different types of spectroscopy studies clearly indicate that the ternary complexes of amino acids are encapsulated in zeolite-Y.

Acknowledgements

The all authors gratefully acknowledged to CSIR (Council of Scientific & Industrial Research) for financial support to do the research. We also thank for the research facilities provided by Nizam College, Osmania University (OU).

Declaration of Interest

The authors declare no conflict of interest.

.

References

[1] Hey, M.H. 1930. Studies on the zeolites part I: general review, Mineral. Mag. 22: 422–437.

[2] F.A. Cotton, G. Wilkinson, Advanced Inorganic Chemistry, 3rd ed., Wiley Eastern, New Delhi, 1993, p. 894.

[3] F. Liebau, Zeolites and clathrasils: two distinct classes of framework silicates, Zeolites 3 (1983) 191–193.

[4] C. Colella, W.S. Wise, The IZA Handbook of Natural Zeolites: a tool of knowledge on the most important family of porous minerals, Microporous Mesoporous Mater. 189 (2014) 4–10.

[5] P.C.H. Mitchel, Zeolite-encapsulated metal complexes: biomimetic catalysts, Chemistry and Industry (6 May) (1991) 308.

[6] C.R. Jacob, S.P. Varkey, P. Ratnasamy, Liquid-Phase Catalytic Hydroxylation of Phenol Using Cu (II), Ni(II) and Zn(II) Complexes of Amidate Ligand Encapsulated in Zeolite-Y as Catalysts, Appl. Catal. A Gen. 168 (1998) 353.

[7] S. Deshpande, D. Srinivas, P. Ratnasamy, EPR and catalytic investigation of Cu (salen) complexes encapsulated in zeolites. J. Catal. 188 (1999) 261.

[8] C. Bowers, P.K. Dutta, Olefin oxidation by zeolite-encapsulated Mn (salen)+ complexes under ambient conditions, J. Catal. 122 (1990) 271.

[9] P.P. Knops Gerrits, D.D. De Vos, F. Thibaut-Starzyk, P.A. Jacobs, Zeolite-encapsulated Mn (II) complexes as catalysts for selective alkene oxidation, Nature 369 (1994) 543.

[10] S.P. Varkey, C.R. Jacob, Selective oxidation of styrene using zeolite encapsulated manganese complexes, Indian J. Chem. A 37 (1998) 407.

[11] C. Ratnasamy, A. Murugkar, S. Padhye, S.A. Pardhy, Zeolite-encapsulated 2-(o-aminophenyl) benzimidazole complexes: synthesis, characterization and catalytic activity, Indian J. Chem. A 35 (1996) 1.

[12] S. Kowalak, R.C. Weiss, K.J. Balkus, AlPO4 Molecular Sieves Modified with Metal Chelate Complexes, J. Chem. Soc., Chem. Commun. (1991) 57.

[13] C.R. Jacob, S.P. Varkey, P. Ratnasamy, Oxidation of para-xylene over zeolite-encapsulated copper and manganese complexes. Appl. Catal. A Gen. 182 (1999) 91.

[14] M. Harimohan, F. L. Urbach, Stereochemistry of tetradentate Schiff base complexes of cobalt (II), Inorg. Chem. 8 (1969) 556.

[15] K.I. Balkus Jr., A.G. Gabrielov, Phenomena and molecular recognition in chemistry, J. Inclusion Phenom. 21 (1995) 159.

[16] K.O. Xavier, J. Chacko, K.K. Mohammed Yusuff, Zeolite-encapsulated Co (II), Ni(II) and Cu(II) complexes as catalysts for partial oxidation of benzyl alcohol and ethylbenzene, Appl. Catal. A Gen. 258 (2004) 251–259.

[17] J. Mehta, S. Dhaka, A.K. Paul, S. Dayananda, A. Deep, Organophosphate hydrolase conjugated UiO-66-NH_2 MOF based highly sensitive optical detection of methyl parathion, Environ. Res. 174 (2019) 46–53.

[18] K.K. Bania, R.C. Deka, Zeolite-Y encapsulated metal picolinato complexes as catalyst for oxidation of phenol with hydrogen peroxide, J. Phys. Chem. C 117 (2013) 11663–11678.

[19] I. Viera, M.H. Torre, E. Kremer, S.B. Etcheverry, E.J. Baran, Infrared spectra of copper (II) complexes of amino acids with hydrophobic residues, Acta Farm. Bonaerense 17 (1998) 213–218.

[20] M. M. Elajaily, Amino Acid Schiff Base Complexes of Mn (II), Co (II), Ni (II), Cu (II) and Cd (II) Transition Metal Ions, Egypt. J. Anal. Chem. 16 (2007) 16.

[21] P.S.N. Reddy, B.V. Agarwala, Synthesis and characterization of new Schiff Base complexes of 2-pyridinecarboxaldehyde and thiosemicarbazides, Synth. React. Inorg. Met.Org. Chem. 17 (1987) 585.

[22] M.S. Masoud, S.A. Abou El-Enein, M.E. Ayad, A.S. Goher, Spectral and magnetic properties of phenylazo-6-aminouracil complexes, Spectrochim. Acta A 60 (2004) 77–87.

[23] F.A. El-Saied, S.A. Abou El-Enein, S.M. Emam, H.A. El-Shater, Synthesis and characterization of Cu (II), Ni (II), Co (II), Mn (II), Zn (II), Ru (III), Hf (IV) and ZrO(II) complexes of 2-thiophenylidene-N-4-methoxy anilinoacetohydrazone, Polish J. Chem. 83 (2009) 1871–1883.

[24] I. Viera, M.H. Torre, E. Kremer, S.B. Etcheverry, E.J. Baran, Infrared spectra of copper (II) complexes of amino acids with hydrophobic residues, Acta Farm. Bonaerense 17 (1998) 213–218.

[25] M. Wei et al. Preparation and thermal decomposition studies of L-tyrosine intercalated MgAl, NiAl and ZnAl layered double hydroxides, J. Phys. Chem. Solids, 67 (2006) 1469–1476.

[26] C. Vaysse, L. Guerlou-Demourgues, C. Delmas, Thermal evolution of carbonate pillared layered hydroxides with (Ni, L) (L = Fe, Co) based slabs: grafting or nongrafting of carbonate anions?Inorg. Chem. 41 (2002) 6905-6911.